Chapter 2
Internal Waves in Two-Layer Sea

2.1 Introduction

Two-layer model of the vertical structure of ocean water, where a layer of water of uniform lower density is located over a layer of uniform higher density, with a sharp interface, is quite realistic for coastal regions. River runoff occupies the upper layer of low density, over the deep layer of much higher salinity, and gradient of salinity (i.e. density) occurs between them. Two-layer model is also applicable when one tries to describe an upper, well-mixed oceanic layer located over deeper water. The thermocline is then fairly abrupt and separates water masses above and below, each of which is almost homogeneous. This scenario is sometimes observed during influx of the saline water from the North Sea to the Baltic Sea (Piechura and Beszczyńska-Möller 2004).

The density gradient layer is unstable and under some impulse, disturbances of the waving form are generated. These disturbances are known as the interfacial internal waves. In the following sections two types of solutions for the interfacial waves are discussed. In Sect. 2.2, it is shown that for the infinitesimal interfacial waves, a simple analytical solutions are possible. The final forms for the wave kinematics parameters and vertical structure of wave velocities have been developed. If the amplitude of interfacial waves is higher, the nonlinear effects become visible. For deep and intermediate waters, the solution is obtained in Sect. 2.3 by applying the Stokes's type expansion in the wave steepness. In the same section, the stable solution of the very well known Korteweg-de Vries equation for long interfacial waves is given. In particular, the solitary and cnoidal type solution are discussed in detail.

2.2 Analytic Solutions for Infinitesimal Interfacial Waves

We consider a simple case of a two-layer ocean when the height over which the density change between the layers is small in comparison with the wavelength. Therefore the termocline can be represented approximately by infinitesimally thin interface.

S.R. Massel, *Internal Gravity Waves in the Shallow Seas*,
GeoPlanet: Earth and Planetary Sciences, DOI 10.1007/978-3-319-18908-6_2

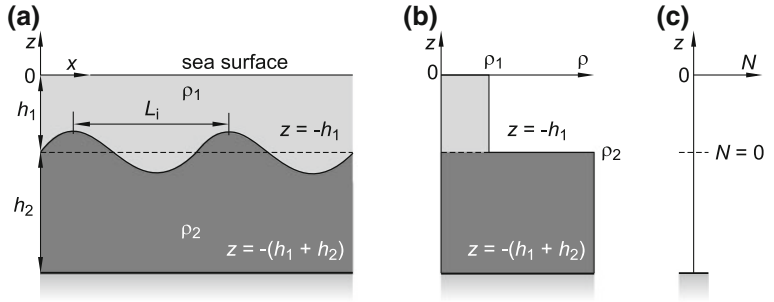

Fig. 2.1 Two-layer ocean model: **a** two layers of fluid of different densities, **b** vertical density profile, **c** vertical profile of frequency (Massel 1999)

We assume that an upper layer of depth h_1 and density ρ_1 is lying on a lower layer of depth h_2 and density ρ_2. The total water depth is equal $h = h_1 + h_2$. An internal wave of frequency ω is propagating at the interface between the layers (see Fig. 2.1). It should be noted that at the level $z = -h_1$, the gradient of water density becomes infinitely large. Thus the Väisälä-Brunt frequency, $N(z)$, cannot be defined at that level, and in both layers, the frequency $N(z)$ is simply equal zero.

Let us assume that $\omega^2 \gg f^2$ and therefore the Earth rotation is neglected. This condition is usually satisfied for relatively short internal waves. For example, for station located at the latitude $\varphi \sim 50°$, and for internal waves period $1/4\,\mathrm{h} < \mathrm{T} < 3\,\mathrm{h}$, the ratio of the inertial frequency f and internal wave frequency ω is $0.016 < (f/\omega) < 0.191$.

If the fluid is irrotational and incompressible in both layers, the governing equations describing the wave motion can be presented in the form of velocity potentials (Sutherland 2010):

$$\left.\begin{aligned} \nabla^2\phi_1 = 0 \text{ for } -h_1 \le z \le 0 \\ \nabla^2\phi_2 = 0 \text{ for } -h \le z \le -h_1 \end{aligned}\right\} \tag{2.1}$$

with the following kinematic and dynamic boundary conditions:

$$\frac{\partial\phi_1}{\partial z} = \frac{\partial\phi_2}{\partial z} = \frac{\partial\zeta}{\partial t} \quad \text{at} \quad z = -h_1 \tag{2.2}$$

and

$$\rho_1 \frac{\partial\phi_1}{\partial t} + \rho_1 g\zeta = \rho_2 \frac{\partial\phi_2}{\partial t} + \rho_2 g\zeta \quad \text{at} \quad z = -h_1 \tag{2.3}$$

$$\frac{\partial\phi_1}{\partial z} = 0 \quad \text{at} \quad z = 0 \tag{2.4}$$

$$\frac{\partial \phi_2}{\partial z} = 0 \quad \text{at} \quad z = -h \tag{2.5}$$

with the interfacial displacement ζ assumed in the form $\zeta(x,t) = A\cos(kx - \omega t)$.

We adopt the velocity potentials ϕ_1 and ϕ_2 to the boundary value problem as follows:

$$\phi_1(x,z,t) = -\frac{\omega}{k} A \frac{\cosh(kz)}{\sinh(kh_1)} \sin(kx - \omega t) \tag{2.6}$$

$$\phi_2(x,z,t) = \frac{\omega}{k} A \frac{\cosh[k(z+h)]}{\sinh(kh_2)} \sin(kx - \omega t) \tag{2.7}$$

Substituting Eqs. (2.6) and (2.7) into Eq. (2.3), we get the dispersion relation and the phase velocity C_0 as follows:

$$\omega^2 = \frac{gk(\rho_2 - \rho_1)}{\rho_1 \coth(kh_1) + \rho_2 \coth(kh_2)} \tag{2.8}$$

and

$$C_0 = \frac{\omega}{k} = \sqrt{\frac{g}{k} \frac{(\rho_2 - \rho_1)}{\rho_1 \coth(kh_1) + \rho_2 \coth(kh_2)}} \tag{2.9}$$

The fluid velocities u and w in both layers can be found from the velocity potentials, i.e.:

– upper layer

$$\left.\begin{aligned} u_1(x,z,t) &= \frac{\partial \phi_1}{\partial x} = -\omega A \frac{\cosh(kz)}{\sinh(kh_1)} \cos(kx - \omega t) = U_1(z)\cos(kx - \omega t) \\ w_1(x,z,t) &= \frac{\partial \phi_1}{\partial z} = -\omega A \frac{\sinh(kz)}{\sinh(kh_1)} \sin(kx - \omega t) = W_1(z)\sin(kx - \omega t) \end{aligned}\right\} \tag{2.10}$$

– lower layer

$$\left.\begin{aligned} u_2(x,z,t) &= \frac{\partial \phi_2}{\partial x} = \omega A \frac{\cosh[k(z+h)]}{\sinh(kh_2)} \cos(kx - \omega t) = U_2(z)\cos(kx - \omega t) \\ w_2(x,z,t) &= \frac{\partial \phi_2}{\partial z} = \omega A \frac{\sinh[k(z+h)]}{\sinh(kh_2)} \sin(kx - \omega t) = W_2(z)\sin(kx - \omega t) \end{aligned}\right\} \tag{2.11}$$

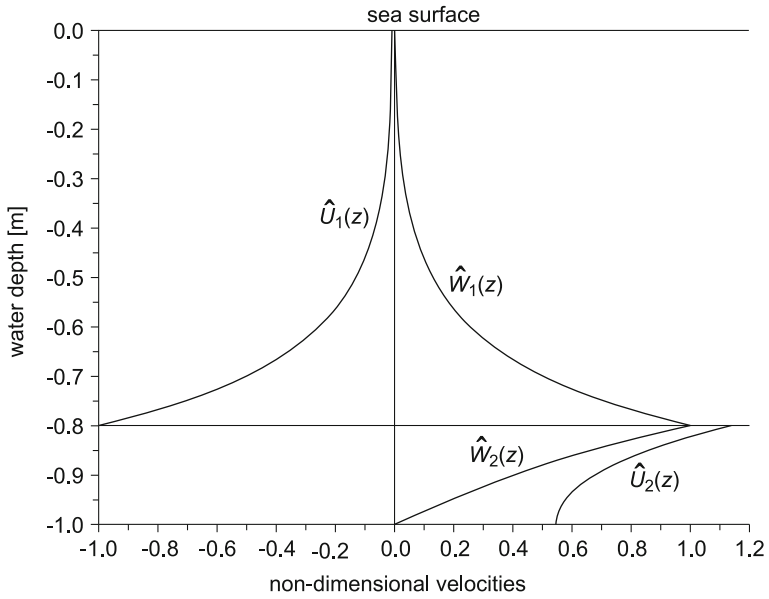

Fig. 2.2 Vertical profiles of non-dimensional velocity amplitudes in two-layer fluid (deep water case)

For illustration, we consider a laboratory experimental case when the total water depth $h = 1.0\,\mathrm{m}$. The water depths and densities in upper and lower layers are equal $h_1 = 0.8\,\mathrm{m}$, $\rho_1 = 1005\,\mathrm{kg\,m^{-3}}$, and $h_2 = 0.2\,\mathrm{m}$, $\rho_2 = 1025\,\mathrm{kg\,m^{-3}}$, respectively. Interfacial wave period is equal $T = 8\,\mathrm{s}$. From Eqs. (2.8) and (2.9) it follows that wavelength $L = 0.919\,\mathrm{m}$ and the phase velocity $C_0 = 0.115\,\mathrm{m}$.

In Fig. 2.2 the vertical profiles of the non-dimensional velocity amplitudes ($\hat{U}(z) = U(z)/\omega A$ and $\hat{W}(z) = W(z)/\omega A$) are shown. The vertical and horizontal velocity amplitudes decay from the interface line to the sea surface and sea bottom. The horizontal velocity amplitude in the lower layer is opposite to that in the upper layer. Please note that in the Fig. 2.2, the horizontal velocity at $z = 0$ does not exactly equal zero but in our case it is equal to $\hat{U}_1(z) = -0.00844$. Let us reconstruct an approximate path followed by an individual fluid parcel during the passage of a small-amplitude internal wave. We assume that parcel motion around a fixed point (x_0, z_0) is small. Therefore, the actual position of parcel $(x(t), z(t))$ at time t is given by:

–upper layer

$$\left.\begin{aligned} x(t) &\approx x_0^{(1)} + \int_0^t u_1 dt \\ z(t) &\approx z_0^{(1)} + \int_0^t w_1 dt \end{aligned}\right\} \tag{2.12}$$

–lower layer

$$\left.\begin{aligned} x(t) &\approx x_0^{(2)} + \int_0^t u_2 dt \\ z(t) &\approx z_0^{(2)} + \int_0^t w_2 dt \end{aligned}\right\} \tag{2.13}$$

Substituting Eqs. (2.10) and (2.11) into Eqs. (2.12) and (2.13) we obtain:
–upper layer

$$\left.\begin{aligned} x(t) &\approx x_0^{(1)} - \frac{U_1\left(z_0^{(1)}\right)}{\omega} \sin\left(kx_0^{(1)} - \omega t\right) \\ z(t) &\approx z_0^{(1)} + \frac{W_1\left(z_0^{(1)}\right)}{\omega} \cos\left(kx_0^{(1)} - \omega t\right) \end{aligned}\right\} \tag{2.14}$$

–lower layer

$$\left.\begin{aligned} x(t) &\approx x_0^{(2)} - \frac{U_2\left(z_0^{(2)}\right)}{\omega} \sin\left(kx_0^{(2)} - \omega t\right) \\ z(t) &\approx z_0^{(2)} + \frac{W_2\left(z_0^{(2)}\right)}{\omega} \cos\left(kx_0^{(2)} - \omega t\right) \end{aligned}\right\} \tag{2.15}$$

Under the assumption of small-amplitude wave, the displacements from the original position are small, so we can approximate $x \sim x_0$ and $z \sim z_0$ on the right-hand sides of Eqs. (2.14) and (2.15).

Eliminating time t in these equations, we obtain the elliptic path of the parcel in the form:

$$\frac{\left(x - x_0^{(1)}\right)^2}{A_1^2} + \frac{\left(z - z_0^{(1)}\right)^2}{B_1^2} = 1 \tag{2.16}$$

and

$$\frac{\left(x - x_0^{(2)}\right)^2}{A_2^2} + \frac{\left(z - z_0^{(2)}\right)^2}{B_2^2} = 1 \tag{2.17}$$

in which:

$$\frac{A_1}{A} = \frac{\cosh\left(kz_0^{(1)}\right)}{\sinh(kh_1)}, \quad \frac{B_1}{A} = \frac{\sinh\left(kz_0^{(1)}\right)}{\sinh(kh_1)} \tag{2.18}$$

$$\frac{A_2}{A} = \frac{\cosh\left[k\left(z_0^{(2)} + h\right)\right]}{\sinh(kh_2)}, \quad \frac{B_2}{A} = \frac{\sinh\left[k\left(z_0^{(2)} + h\right)\right]}{\sinh(kh_2)} \tag{2.19}$$

The orbit dimensions close to the interface are:

$$\frac{A_1}{A} = \frac{A_2}{A} \sim \coth(kh_1), \quad \frac{B_1}{A} = \frac{B_2}{A} \sim 1.0 \tag{2.20}$$

and they decay from the interface; namely, close to the sea surface we have:

$$\frac{A_1}{A} \sim \frac{1}{\sinh(kh_1)} \quad \text{and} \quad \frac{B_1}{A} \sim 0 \tag{2.21}$$

while close to sea bottom they become:

$$\frac{A_2}{A} \sim \frac{1}{\sinh(kh_2)} \quad \text{and} \quad \frac{B_2}{A} \sim 0 \tag{2.22}$$

All formulae for wave velocity amplitudes and dispersion relation for some combinations of the water depths h_1 and h_2 can be simplified. In particular, for the deep water waves when $kh_1 \gg 1$ and $kh_2 \gg 1$, the dispersion relation and phase velocity are as follows:

$$\omega = \sqrt{gk\frac{\rho_2 - \rho_1}{\rho_2 + \rho_1}} = \varepsilon\sqrt{gk}, \quad C_0 = \varepsilon\sqrt{\frac{g}{k}} \tag{2.23}$$

where:

$$\varepsilon = \sqrt{\frac{\rho_2 - \rho_1}{\rho_2 + \rho_1}} \tag{2.24}$$

The quantity ε is a small number if density difference between the two layers is small. From Eq. (2.23) it follows that waves at the interface between two liquids of infinite thickness travel like deep water surface waves, but at a much reduced frequency due to small parameter ε. Consequently, the phase speed will be much smaller than speed of surface waves. For example, if $\rho_1 = 1020\,\mathrm{kg\,m^{-3}}$ and $\rho_2 = 1023\,\mathrm{kg\,m^{-3}}$, Eq. (2.23) gives:

$$C_0 = 0.038\sqrt{\frac{g}{k}} = 0.038C \tag{2.25}$$

where C is the phase velocity of the surface wave of this length.

On the other hand, for shallow water long waves, when $kh_1 \ll 1$ and $kh_2 \ll 1$, the phase velocity becomes:

$$C_0 = \sqrt{\frac{g(\rho_2 - \rho_1)\, h_1 h_2}{\rho_2 h_1 + \rho_1 h_2}} \tag{2.26}$$

Let us assume that densities ρ_1 and ρ_2 are the same as above, and additionally $h_1 = h_2$. Thus, Eq. (2.26) gives:

$$C_0 = \varepsilon\sqrt{gh_2} = \varepsilon C = 0.038C \tag{2.27}$$

Again the phase speed of an internal wave is much smaller than that of a long surface wave of this length. These waves are non-dispersive and travel slowly because of small density difference.

In the coastal regions, near river estuaries, the upper layer is usually very thin, say $kh_1 \ll 1$, over a deep lower layer, where usually $kh_2 \gg 1$. Using these water depth conditions in Eq. (2.9), we obtain:

$$C_0 \approx \sqrt{\frac{\rho_2 - \rho_1}{\rho_1}\, gh_1} \tag{2.28}$$

For example, if $h_1 = 5\,\mathrm{m}$, $\rho_1 = 1000\,\mathrm{kg\,m^{-3}}$ (fresh water), and $\rho_2 = 1023\,\mathrm{kg\,m^{-3}}$ (salt water), the phase velocity, C_0, becomes $0.15\sqrt{gh_1} = 1.05\,\mathrm{m\,s^{-1}}$.

For shallow water, when $kh_1 \ll 1$ and $kh_2 \ll 1$, both components of the internal wave velocities become approximately linear functions of z coordinate. From Eqs. (2.10) and (2.11) we obtain the amplitudes of velocities in the form:

– upper layer

$$\left.\begin{aligned} U_1(z) &= -\omega A\,\frac{\cosh(kz)}{\sinh(kh_1)} \approx -\frac{\omega A}{kh_1} = -\frac{AC_0}{h_1} \\ W_1(z) &= -\omega A\,\frac{\sinh(kz)}{\sinh(kh_1)} \approx -\omega A\frac{z}{h_1} = -\frac{AC_0}{h_1}\,(kz) \end{aligned}\right\} \tag{2.29}$$

– lower layer

$$\left.\begin{aligned} U_2(z) &= \omega A\,\frac{\cosh[k(z+h)]}{\sinh(kh_2)} \approx \frac{\omega A}{kh_2} = \frac{AC_0}{h_2} \\ W_2(z) &= \omega A\,\frac{\sinh[k(z+h)]}{\sinh(kh_2)} \approx \frac{\omega A}{h_2}(z+h) = \frac{AC_0}{h_2}\,k(z+h) \end{aligned}\right\} \tag{2.30}$$

In Fig. 2.3 the vertical profiles of the non-dimensional amplitudes $\hat{U}(z) = U(z)/\omega A$ and $\hat{W}(z) = W(z)/\omega A$ are illustrated for the case of shallow water. The interface is

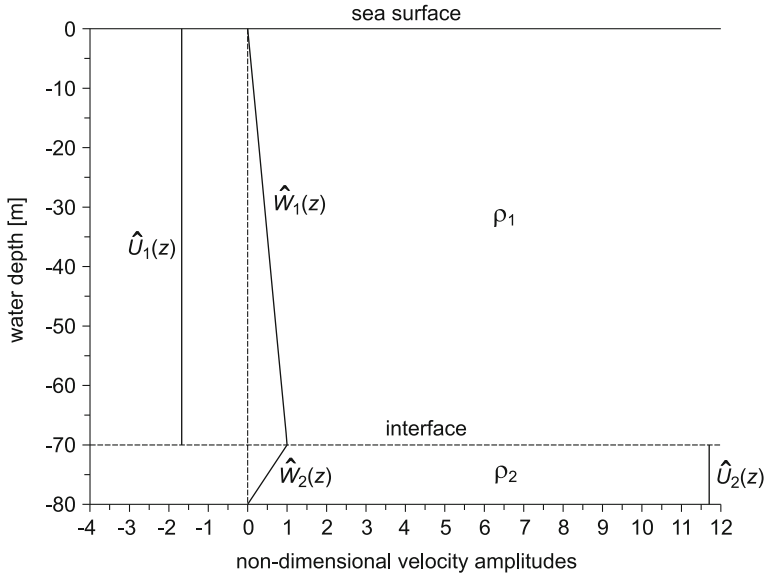

Fig. 2.3 Vertical profiles of non-dimensional velocity amplitudes in two-layer fluid (shallow water case)

located at the water depth $h_1 = 70\,\mathrm{m}$ and the densities of the upper and lower layers are $1004\,\mathrm{kg\,m^{-3}}$ and $1012\,\mathrm{kg\,m^{-3}}$, respectively. The internal wave of amplitude A, period $T = 15\,\mathrm{min}$ ($\omega = 0.00698\,\mathrm{rad\,s^{-1}}$) and wavelength $L = 736\,\mathrm{m}$ ($k = 0.00854\,\mathrm{m^{-1}}$) propagates along the interface with phase velocity $C_0 = 0.818\,\mathrm{m\,s^{-1}}$. The vertical velocity amplitude is a linear function of z with discontinuous gradient at the interface line. The horizontal velocity amplitude does not decay with depth and in the lower layer it is opposite to that in the upper layer.

We also note that internal waves in the ocean produce only a very small vertical displacements of free surface; usually they are smaller by a factor of the order $(\rho_2 - \rho_1)/\rho_1$ (say $\sim 10^{-3}$) than the internal wave displacement.

Suppose now that an object is located at water depth $z = -h_1$ (see Fig. 2.1). This object can be stationary when the balance between its weight and the buoyancy force is maintained. However, due to propagation of the interfacial waves, the object's buoyancy varies depending on the density of the surrounding fluid. In his book Pinet (1992) remarked the nuclear submarine *U.S.S. Thresher*, which was lost in the West Atlantic in 1963 with all crew members. There had been no indication of equipment malfunction or unusual storm weather. As submerged submarines attain neutral buoyancy by flooding or jettisoning sea water from ballast tanks, there are speculations that *U.S.S. Thresher* was probably cruising along a pycnocline when it encountered a large internal wave and suddenly dropped to a greater depth because of the lower density of the ambient water. Evidently the incident occurred too rapidly and the submarine crew was not able to arrest the ship's fall.

2.3 Progressive Interfacial Waves of Finite Amplitude

2.3.1 Deep and Intermediate Waters

Solutions discussed in the previous section are valid under the assumption of infinitesimal waves when the higher order terms are neglected. Here we consider waves of permanent form and finite amplitude propagating at the interface between two fluids of finite depths. Let the wavelength, L, be not too much greater than the fluid depth. For such case, Hunt (1961) provided the third order solution for two-fluid system of finite depths and bounded by upper and bottom rigid horizontal planes. The shape of the interfacial wave is:

$$\begin{aligned}\zeta(x,t) = {} & A_1 \cos(kx - \omega t) + A_2 \cos 2(kx - \omega t) + \\ & + A_3 \cos 3(kx - \omega t)\end{aligned} \tag{2.31}$$

where A_1, A_2 and A_3 are the amplitudes of components of first, second and third order, respectively. The symbols k and ω denote the wavenumber and wave frequency.

For amplitudes A_2 and A_3 we have (Thorpe 1968):

$$A_2 = \frac{A_1(kA_1)}{4}\left[\rho_2\frac{(3-T_2)^2}{T_2^2} - \rho_1\frac{(3-T_1)^2}{T_1^2}\right](\rho_1 T_1 + \rho_2 T_2)^{-1} \tag{2.32}$$

and

$$A_3 = \frac{kA_1}{16}\left(S_{31}A_2 - S_{32}(kA_1)A_1\right)S_{33}^{-1} \tag{2.33}$$

$$S_{31} = \frac{9 + 4T_2^2 + 3T_2^4}{T_2^2(3+T_2^2)}\rho_2 - \frac{9 + 4T_1^2 + 3T_1^4}{T_2^2(3+T_1^2)}\rho_1 \tag{2.34}$$

$$S_{32} = \frac{3 - T_2^2}{T_2^2(3+T_2^2)}\rho_2 + \frac{3 - T_1^2}{T_1^2(3+T_1^2)}\rho_1 \tag{2.35}$$

$$S_{33} = \frac{\rho_1 T_1}{3 + T_1^2} + \frac{\rho_2 T_2}{3 + T_2^2} \tag{2.36}$$

with:

$$T_1 = \tanh(kh_1), \quad T_2 = \tanh(kh_2) \tag{2.37}$$

The equations above are simplified for particular water depths. If depths of upper and lower layers are the same ($h_1 = h_2 = h$), the amplitudes A_2 and A_3 become as

follows (Thorpe 1968):

$$A_2 = \frac{1}{4} A_1(kA_1) \frac{\rho_2 - \rho_1}{\rho_1 + \rho_2} \frac{3 - T^2}{T^3} \tag{2.38}$$

$$A_3 = \frac{1}{64} A_1(kA_1)^2 \frac{3 - T^2}{T^6} S_{34} \tag{2.39}$$

where:

$$S_{34} = \frac{(\rho_2 - \rho_1)^2 (9 + 4T^2 + 3T^4) - 4(\rho_1 + \rho_2)^2 T^2}{(\rho_1 + \rho_2)^2} \tag{2.40}$$

$$T = \tanh(kh) \tag{2.41}$$

The corresponding dispersion relation is:

$$\omega^2 = gkT \frac{\rho_2 - \rho_1}{\rho_1 + \rho_2} S_d \tag{2.42}$$

where:

$$S_d = 1 + \frac{(kA_1)^2}{8T^4(\rho_1 + \rho_2)} \left[4(\rho_1 + \rho_2)^2 T^2 (2T^2 - 1) + (\rho_2 - \rho_1)^2 (3 - T^2) \right] \tag{2.43}$$

Now we remove the rigid upper boundary and express the fluid surface with accuracy to the second order as follows (Thorpe 1968):

$$\zeta_s(x, t) = a_1 \cos(kx - \omega t) + a_2 \cos 2(kx - \omega t) \tag{2.44}$$

while the equation of the interface displacement to the second order becomes:

$$\zeta(x, t) = A_1 \cos(kx - \omega t) + A_2 \cos 2(kx - \omega t) \tag{2.45}$$

The amplitudes A_1, A_2 and a_1, a_2 are given by Thorpe (1968), and the dispersion relation is:

$$\omega^4(\rho_1 T_1 T_2 + \rho_2) - \omega^2 gk\rho_2(T_1 + T_2) + (\rho_2 - \rho_1) T_1 T_2 (gk)^2 = 0 \tag{2.46}$$

A sufficient condition for the motion of the upper surface to be neglected is:

$$\cosh(kh_1) \frac{\rho_2 - \rho_1}{\rho_2} \frac{\tanh(kh_1)}{\tanh(kh_1) + \tanh(kh_2)} \tag{2.47}$$

If the above inequality becomes true, we may suppose that the fluid has a fixed horizontal boundary as it was considered by Hunt (1961) (see Eq. 2.31).

A special type of distortion of the interface shape appears when kh_2 is large while kh_1 remains small, and the density difference is small. From Eqs. (2.31) and (2.32) we obtain (Thorpe 1968):

$$\zeta(x,t) = A_1 \cos(kx - \omega t) - \frac{3}{4} A_1 (kA_1) \left(\frac{1 - T_1}{T_1^2} \right) \cos 2(kx - \omega t) \tag{2.48}$$

In this profile, the troughs are narrower than the crests, just opposite to the free surface waves in a homogeneous fluid.

If kh_1 is large and the density difference between the fluids is small again, the interface shape becomes:

$$\zeta(x,t) = A_1 \cos(kx - \omega t) + \frac{3}{4} A_1 (kA_1) \left(\frac{1 - T_2}{T_2^2} \right) \cos 2(kx - \omega t) \tag{2.49}$$

which is similar to the surface gravity wave.

In general, when the fluid is bounded by a rigid surface above, the crests of wave profile may be narrower or wider than the troughs depending on whether $\rho_2(3 - T_2^2)/T_2^2$ is greater or less than $\rho_1(3 - T_1^2)/T_1^2$.

The extension of the second-order solution for the random internal waves propagating in a two-layer fluid was considered by Song (2004). He used a methodology of Sharma and Dean (1979) to discuss both the progressive and standing waves. When the upper surface of the two-layer fluid is free, the second-order solution for random internal waves and surface waves was developed by Liu (2006).

2.3.2 Long Interfacial Waves

2.3.2.1 General Remarks

If the wavelength of the internal waves is significantly longer than the characteristic fluid depth, the linear waves are non-dispersive with z-independent horizontal velocity and linear variation with z of the vertical velocity. However, when wave amplitude A is not too small, the weakly nonlinear effect produces wave different from the sinusoidal wave shape by wave crests steepening. Moreover, if the horizontal extent of waves is not too long, compared to the fluid depth h, the weak dispersion appears, broadening the waves. In most efforts to describe the evolution of these waves the Kortweg-de Vries (KdV) theory (Korteweg and de Vries 1895;

Miles 1981) is usually applied. In this theory, a balance between nonlinearity and dispersion of waves is parameterized by two nonlinear variables:

$$\alpha = \frac{A}{h}, \quad \beta = \left(\frac{h}{l}\right)^2 \tag{2.50}$$

where A is the wave amplitude and l is the wavelength scale. For this balance, both parameters must be of the same order of magnitude and both small, i.e. $\beta = O(\alpha) \ll 1$. If these two effects are balanced, solution of the Korteweg-de Vries equation results in steady waves such as solitary waves or cnoidal waves (Whitham 1974; Miles 1981; Massel 1989).

To exploit further the nonlinear and dispersive properties of the solitary and cnoidal internal waves, an extension of the Korteweg-de Vries (KdV) equation, known as the extended KdV (eKdV) equation or Gardner equation including cubic nonliearity is employed (Helfrich and Melville 1986, 2006; Grimshaw et al. 2007; Pelinovsky et al. 1994, 2007):

$$\frac{\partial \zeta}{\partial t} + (C_0 + \alpha\zeta + \alpha_1\zeta^2)\frac{\partial \zeta}{\partial x} + \beta\frac{\partial^3 \zeta}{\partial x^3} = 0 \tag{2.51}$$

in which ζ is the displacement of the interfacial wave and the linear phase velocity C_0 is the eigenvalue of the Sturm-Louville problem for the eigenmode. The coefficients α, α_1 and β are functions of the vertical stratification of fluid under the Boussinesq approximation.

To apply the extended KdV (eKdV) equation for the interfacial waves propagating in a two-layer fluid we define coefficients α, α_1 and β as follows (Helfrich and Melville 2006):

$$C_0 = \sqrt{\left(\frac{g\sigma h_1 h_2}{h_1 + h_2}\right)} \tag{2.52}$$

$$\alpha = \frac{3}{2}C_0\frac{h_1 - h_2}{h_1 h_2} \tag{2.53}$$

$$\alpha_1 = \frac{3C_0}{(h_1 h_2)^2}\left[\frac{7}{8}(h_1 - h_2)^2 - \left(\frac{h_1^3 + h_2^3}{h_1 + h_2}\right)\right] \tag{2.54}$$

$$\beta = \frac{C_0}{6}h_1 h_2 \tag{2.55}$$

where relative layer density difference $\sigma = 2(\rho_2 - \rho_1)/(\rho_1 + \rho_2) \ll 1$. The parameter β is always positive, the nonlinear parameter α however can be either positive or negative. If depth layer $h_1 = h_2$, and parameter $\alpha = 0$, it is necessary also to take into account the cubic nonlinearity. When $h_1 > h_2$, the pycnocline is displaced

upward, in the opposite case ($h_2 > h_1$), the internal wave changes polarity and the depression of pycnocline is observed. This phenomenon was clearly illustrated by Lien et al. (2014) and Grimshaw et al. (2014) for internal solitary waves in the South China Sea. The effect of the change in sign of α on internal solitary waves leads to complex pictures of nonlinear transformation, including breaking of solitons and shocks on both the front and back faces of the waves. General relations for the coefficients with continuous stratification and shear fluid flow have been discussed by Grimshaw et al. (2004)—see also Chap. 3.

2.3.2.2 Solitary Waves

When α_1 is set to zero, Eq. (2.51) reduces to the classical KdV equation:

$$\frac{\partial \zeta}{\partial t} + C_0 \frac{\partial \zeta}{\partial x} + \alpha \zeta \frac{\partial \zeta}{\partial x} + \beta \frac{\partial^3 \zeta}{\partial x^3} = 0 \tag{2.56}$$

Let us find the stable solutions of this equation for the case when interfacial waves are propagating in a constant water depth. We first transform Eq. (2.51) to a frame moving at some constant speed U. Thus we can write $\zeta(x, t) = \zeta(X) = \zeta(x - Ut)$. After substituting this representation into Eq. (2.51), multiplying by $(\partial\zeta/\partial X)$ and integrating we obtain:

$$\left(\frac{\partial \zeta}{\partial X}\right)^2 + \frac{\hat{\alpha}}{3\hat{\beta}} \zeta^3 - \left(\frac{U}{C_0} - 1\right) \frac{1}{\hat{\beta}} \zeta^2 + \left(\frac{2}{C_0 \hat{\beta}} D_1\right) \zeta + \left(\frac{2}{C_0 \hat{\beta}} D_2\right) = 0 \tag{2.57}$$

in which D_1 and D_2 are integration constants, and

$$\hat{\alpha} = \frac{\alpha}{C_0}, \quad \hat{\beta} = \frac{\beta}{C_0} \tag{2.58}$$

The solitary wave, which is one of the possible solutions of the KdV equation, requires that displacement ζ and its derivatives tend to zero at infinity. Thus $D_1 = D_2 = 0$, and Eq. (2.57) takes the form (Whitham 1974):

$$\frac{3\hat{\beta}}{\hat{\alpha}} \left(\frac{d\zeta}{dX}\right)^2 = \zeta^2 (A - \zeta) \tag{2.59}$$

in which the amplitude A (maximum vertical displacement above the equilibrium fluid level) is:

$$A = \frac{3}{\hat{\alpha}} \left(\frac{U}{C_0} - 1\right) \tag{2.60}$$

and the solitary wave speed is:

$$U = C_0\left(1 + \frac{\hat{\alpha}}{3}A\right) = C_0\left(1 + \frac{1}{2}\frac{h_1^2 - h_2^2}{h_1 h}\frac{A}{h_2}\right) \tag{2.61}$$

From Eq. (2.59), the shape of the solitary wave becomes:

$$\zeta(x,t) = A\cosh^{-2}\left[\left(\frac{\hat{\alpha}A}{12\hat{\beta}}\right)^{1/2}(x - Ut)\right] \tag{2.62}$$

or

$$\zeta(x,t) = A\cosh^{-2}\left\{\sqrt{\frac{3A}{4hh_2^2}\left[1 - \left(\frac{h_2}{h_1}\right)^2\right]}(x - Ut)\right\} \tag{2.63}$$

Let us define the characteristic water depth h_r as follows:

$$h_{\mathrm{r}}^3 = hh_2^2\left[1 - \left(\frac{h_2}{h_1}\right)^2\right]^{-1} \tag{2.64}$$

Thus we can represent the solitary internal wave in the classical form:

$$\zeta(x,t) = A\cosh^{-2}\left\{\sqrt{\frac{3A}{4h_{\mathrm{r}}^3}}(x - Ut)\right\} \tag{2.65}$$

The horizontal velocities induced by the internal wave for both layers are equal, respectively (Zheng et al. 2001):

$$u_1(x,t) = -\frac{AC_0}{h_1}\cosh^{-2}\left\{\sqrt{\frac{3A}{4h_{\mathrm{r}}^3}}(x - Ut)\right\} \tag{2.66}$$

and

$$u_2(x,t) = \frac{AC_0}{h_2}\cosh^{-2}\left\{\sqrt{\frac{3A}{4h_{\mathrm{r}}^3}}(x - Ut)\right\} \tag{2.67}$$

It should be noted that the solution of the extended KdV equation (eKdV) Eq. (2.51) for solitary wave takes the form (Helfrich and Melville 2006):

$$\zeta(x,t) = \frac{A}{b + (1-b)\cosh^2[\gamma(x - Ut)]} \tag{2.68}$$

in which:

$$U = C_0 + \frac{A}{3}\left(\alpha + \frac{1}{2}\alpha_1 A\right), \quad \gamma^2 = \frac{A\left(\alpha + \frac{1}{2}\alpha_1 A\right)}{12\beta}, \quad b = \frac{-A\alpha_1}{2\alpha + \alpha_1 A} \tag{2.69}$$

2.3.2.3 Cnoidal Waves

Except for the solitary wave, another permanent form of the long internal wave profile exists, being also a solution of the KdV equation. This solution is described by the elliptic function $cn(\theta; m)$ and it is known as the cnoidal wave. The length of the cnoidal wave is limited, thus in Eq. (2.57), both constants D_1, D_2 should be different from zero. Therefore we have:

$$\frac{3\hat{\beta}}{\hat{\alpha}}\left(\frac{\partial\zeta}{\partial x}\right)^2 = -\zeta^3 + \frac{3}{\hat{\alpha}}\left(\frac{U}{C_0} - 1\right)\zeta^2 - \left(\frac{6}{C_0\hat{\alpha}}\right)D_1 - \zeta + \\ + \left(\frac{6}{C_0\hat{\alpha}}\right)D_2 = (\zeta_3 - \zeta)(\zeta - \zeta_2)(\zeta - \zeta_1) = P_3 \tag{2.70}$$

in which $\zeta_1 < \zeta_2 < \zeta_3$ are zeros of the third-order polynomial P_3. In particular, ζ_3 and ζ_2 correspond to the heights of the crest and trough, respectively, and the difference $\zeta_3 - \zeta_2 = H$ is equal the total wave height. Following Mei et al. (2005) we find:

$$\zeta_1 = -\frac{H}{m}\frac{\mathbf{E}}{\mathbf{K}} \tag{2.71}$$

$$\zeta_2 = \frac{H}{m}\left(1 - \frac{\mathbf{E}}{\mathbf{K}} - m\right) \tag{2.72}$$

$$\zeta_3 = \frac{H}{m}\left(1 - \frac{\mathbf{E}}{\mathbf{K}}\right) \tag{2.73}$$

where $\mathbf{K}$ and $\mathbf{E}$ are the complete elliptic integrals of the first and second kind, respectively (Abramowitz and Stegun 1975):

$$\mathbf{K}(m) = \int_0^{\pi/2} \frac{du}{\sqrt{1 - m\sin^2 u}} \tag{2.74}$$

and

$$\mathbf{E}(m) = \int_0^{\pi/2} \sqrt{1 - m\sin^2 u}\, du \tag{2.75}$$

in which m is the parameter of the elliptic functions and integrals, such that $m = (\zeta_3 - \zeta_2)/(\zeta_3 - \zeta_1), 0 \le m \le 1$. In practice, the parameter m is not known "a priori" but must be obtained as a function of wave height H, wavelength L (or wave period T) and water depth h.

The solution of the KdV equation now becomes:

$$\begin{aligned}\zeta(x,t) &= \zeta_2 + Hcn^2\left[\left(\frac{\hat{\alpha}}{12\hat{\beta}}\right)^{1/2}(\zeta_3-\zeta_1)^{1/2}(x-Ut)\right] = \\ &= \frac{H}{m}\left(1-\frac{\mathbf{E}}{\mathbf{K}}-m\right) + Hcn^2\left[\left(\frac{\hat{\alpha}}{12\hat{\beta}}\right)^{1/2}\left(\frac{H}{m}\right)^{1/2}(x-Ut)\right] = \\ &= \frac{H}{m}\left(1-\frac{\mathbf{E}}{\mathbf{K}}-m\right) + Hcn^2\left[\frac{2\mathbf{K}(m)}{L}(x-Ut)\right] \end{aligned} \tag{2.76}$$

in which $cn(x,t;m)$ is the cosine-elliptic function which is, by definition, periodic with x with the period $4\mathbf{K}$ (Abramowitz and Stegun 1975).

Since $cn^2(x,t;m)$ must have the period $2\mathbf{K}(m)$, the wavelength L is:

$$L = \left(\frac{48\hat{\beta}}{\hat{\alpha}}\right)^{1/2}\left(\frac{m}{H}\right)^{1/2}\mathbf{K}(m) \tag{2.77}$$

or

$$L^2 = \frac{16}{3}\frac{h_r^3}{H}m\mathbf{K}^2(m) \tag{2.78}$$

and

$$\left(\frac{H}{h_r}\right)\left(\frac{L}{h_r}\right)^2 = \frac{16}{3}m\mathbf{K}^2(m) \tag{2.79}$$

which are transcendental relationships for unknown parameter m. For cnoidal wave speed we have:

$$U = C_0\left\{1+\frac{\hat{\alpha}H}{3m}\left[2-3\frac{\mathbf{E}}{\mathbf{K}}-m\right]\right\} \tag{2.80}$$

or

$$U = C_0\left\{1+\frac{1}{2}\frac{h_1-h_2}{h_1h_2}\left(\frac{H}{m}\right)\left[2-3\frac{\mathbf{E}}{\mathbf{K}}-m\right]\right\} \tag{2.81}$$

When $m \to 1$, we have $\mathbf{K}(1) = \infty$, $\mathbf{E}(1) = 1$. Thus $\zeta_2 \to \zeta_1$, $L \to \infty$ and $cn^2(x) \to \cosh^{-2}(x)$. Taking into account that the ratio $\mathbf{K}/L$ approaches a finite

limit (see Eq. 2.77), from Eq. (2.76) we get the solitary wave profile:

$$\zeta(x,t) = H\cosh^{-2}\left\{\sqrt{\frac{3H}{4h_1^3}}(x-Ut)\right\} \tag{2.82}$$

which is equivalent to Eq. (2.65) when we use $H = A$.

From Eq. (2.80) for $m \to 1$ it follows that the wave speed U simplifies to Eq. (2.61) as for the solitary waves should be.

In the second limiting case when $m \to 0$, we have $\zeta_3 - \zeta_2 = H \to 0$, $\mathbf{K} = \mathbf{E} = \pi/2$, $U \to C_0$, $cn(u;m) \to \cos(u)$ and $\zeta_2 = -H/2$. Therefore:

$$\zeta = \frac{H}{2}\cos\left[\frac{2\pi}{L}(x - C_0 t)\right] = A\cos(kx - \omega t) \tag{2.83}$$

In Fig. 2.4 the surface elevations of the solitary wave (a) and cnoidal internal wave (b) are illustrated for the following wave parameters: wave height $H = 5\,\mathrm{m}$, wavelength $L = 500\,\mathrm{m}$, water depth $h = 80\,\mathrm{m}$, depth of interface $h_1 = 70\,\mathrm{m}$, and densities of the upper and lower layer $\rho_1 = 1004\,\mathrm{kg\,m^{-3}}$, $\rho_2 = 1012\,\mathrm{kg\,m^{-3}}$, respectively. The resulting wave parameters become: the reduced depth $h_r = 20.14\,\mathrm{m}$ (see Eq. 2.64), linear wave speed $C_0 = 0.81\,\mathrm{m\,s^{-1}}$, wave speed $U = 1.41\,\mathrm{m\,s^{-1}}$ (for cnoidal wave), depth of wave trough $\zeta_2 = -0.94\,\mathrm{m}$ and wave period $T = 354\,\mathrm{s}$.

Till now we have not discussed the breaking of the long waves. However, Grue et al. (2000) developed a fully nonlinear two-layer model where a thin layer of linearly stratified fluid has constant Väisälä-Brunt frequency and a thick layer has zero Väisälä-Brunt frequency. Particular attention was paid to the role of the breaking of waves. For large waves, the breaking occurs in a region in the centre of the waves, and breaking limits the fluid velocity. The experimental and theoretical velocities exhibit a good agreement up to breaking. The maximal amplitude in the experiments was about 1.25 times the depth of the linearly stratified layer, and the maximal propagation speed was approximately 1.78 times the linear long wave speed.

Two-layer model of internal waves described in this chapter should be considered only as an approximation to the real vertical distribution density. In general, the observations in natural conditions showed that the vertical distribution of water density is an arbitrary function of vertical coordinate z. Sometimes, for practical purposes, the following characteristic parameters of the two-layer stratification are used:

$$\chi = \frac{h_p}{h}, \quad \sigma = \frac{\Delta}{\rho_0} \tag{2.84}$$

in which h_p is the scale of thickness of the pycnocline, $\Delta = \rho_2 - \rho_1$, and ρ_0 is the reference density. The parameter χ is known as the Boussinesq parameter. If $\chi \ll 1$, the system is nearly two-layered. Usually in the natural conditions, the parameter χ is much bigger, maybe except the laboratory experiments, and the system should be considered as multi-layered, as is shown in the next chapter.

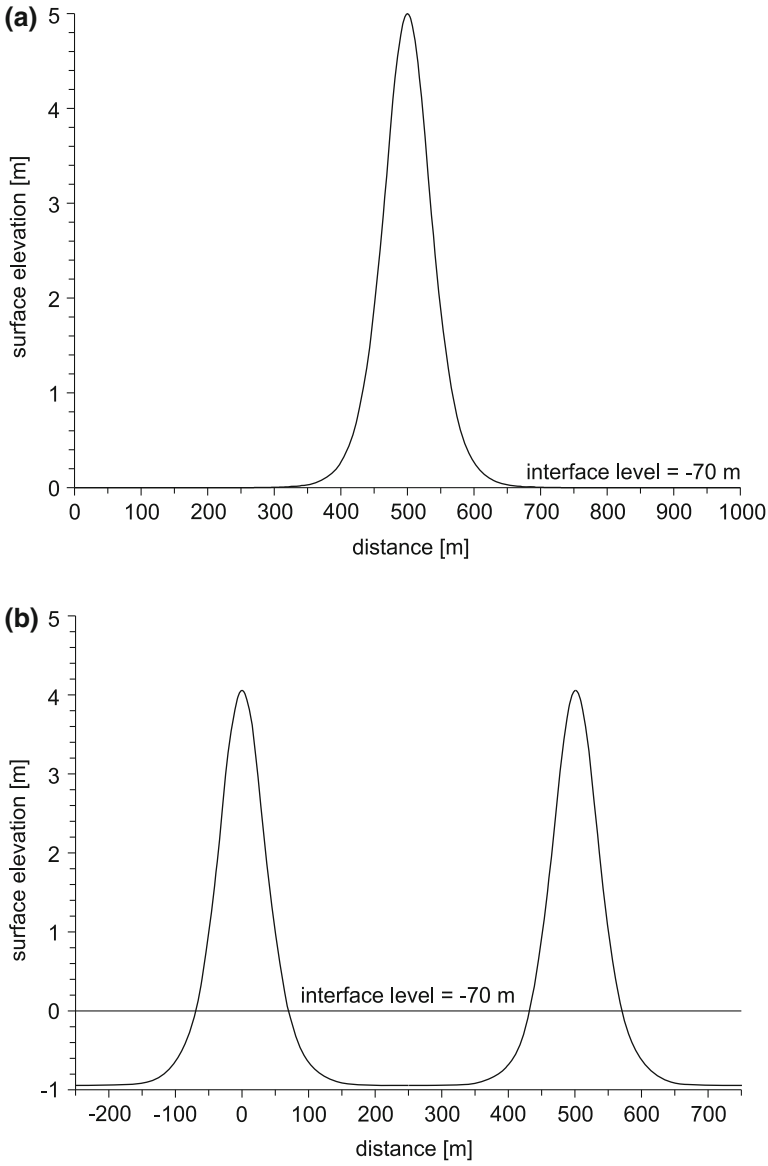

Fig. 2.4 Surface elevations of solitary (**a**) and cnoidal waves (**b**) of the same wave height

References

Abramowitz M, Stegun IA (1975) Handbook of mathematical functions. Dover Publications, New York, 1045 p
Grimshaw R, Pelinovsky E, Talipova T, Kurkin A (2004) Simulation of the transformation of internal solitary waves on oceanic shelves. J Phys Oceanogr 34(12):2774–2791
Grimshaw R, Pelinovsky E, Talipova T (2007) Modelling internal solitary waves in the coastal ocean. Surv Geophys 28:273–298
Grimshaw R, Guo C, Helfrich K, Vlasenko V (2014) Combined effect of rotation and topography on shoaling oceanic internal solitary waves. J Phys Oceanogr 44(4):1116–1132
Grue J, Jensen A, Rusas POV, Sveen JK (2000) Breaking and broadening of internal solitary waves. J Fluid Mech 413:181–217
Helfrich KR, Melville WK (1986) On long nonlinear internal waves over slope-shelf topography. J Fluid Mech 167:285–308
Helfrich KR, Melville WK (2006) Long nonlinear waves. Annu Rev Fluid Mech 38:395–425
Hunt JN (1961) Interfacial waves of finite amplitude. La Houille Blanche 4:515–531
Korteweg DJ, de Vries G (1895) On the change of form of long waves advancing in a rectangular canal, and on a new type of long stationary waves. Phil Mag and J Science 39:422–443
Lien RC, Henyey F, Ma B (2014) Large-amplitude internal solitary waves observed in the Northern South China Sea: properties and energetics. J Phys Oceanogr 44(4):1095–1115
Liu C-M (2006) Second-order random internal and surface waves in a two-fluid system. Geophys Res Lett 33:L06610
Massel SR (1989) Hydrodynamics of coastal zones. Elsevier, Amsterdam, 336 p
Massel SR (1999) Fluid mechanics for marine ecologists. Springer, Berlin, 566 p
Mei CC, Stassine M, Yue DK-P (2005) Theory and applications of ocean surface waves. World Scientific Publishing, Singapore, 1071 p
Miles JW (1981) The Korteweg-de Vries equation: a historical essay. J Fluid Mech 106:131–147
Pelinovsky E, Talipova T, Stepanyants Yu (1994) Modelling of nonlinear wave propagation in the horizontally inhomogeneous ocean. Fizika Atm i Okeana 30:79–85 (in Russian)
Pelinovsky E, Poluhina O, Slunyaev A (2007) Solitary waves in fluids. In: Grimshaw R (ed) Internal solitary waves. WIT Press, Southampton, pp 85–110
Piechura J, Beszczyńska-Möller A (2004) Inflow waters in the deep regions of the southern Baltic Sea-transport and transformations. Oceanologia 46(1):113–141
Pinet PR (1992) Oceanography: an introduction to the planet oceans. West Publishing Company, New York, 571 p
Sharma JN, Dean RG (1979) Development and evaluation of a procedure for simulating a random directional second order sea surface and associated wave forces, vol 20, Ocean Engineering Report University of Delaware, Newark
Song J-B (2004) Second-order random wave solutions for internal waves in a two-layer fluid. Geophys Res Lett 31:L15302
Sutherland B (2010) Internal gravity waves. Cambridge University Press, Cambridge, 377 p
Thorpe SA (1968) On the shape of progressive internal waves. Philos T Roy Soc A 263:563–614
Whitham GB (1974) Linear and nonlinear waves. Wiley, New York, 636 p
Zheng Q, Klemas V, Yan XH, Pan J (2001) Nonlinear evolution of ocean internal solitons propagating along an inhomogeneous thermocline. J Geophys Res 106(C7):14083–14094

http://www.springer.com/978-3-319-18907-9

Internal Gravity Waves in the Shallow Seas
Massel, S.R.
2015, XVI, 163 p. 55 illus., 10 illus. in color., Hardcover
ISBN: 978-3-319-18907-9